CHARACTERIZATION OF TENSILE BEHAVIOR IN UHPFRC THIN SLAB USING NDT METHOD AND DIC SYSTEM

Xiujiang Shen [(1)], and Eugen Brühwiler [(1)]

(1) EPFL – Swiss Federal Institute of Technology, Lausanne, Switzerland

Abstract

Proper test and analysis methods are necessary for characterizing the tensile behavior of strain hardening Ultra High Performance Fiber Reinforced Cementitious Composites (UHPFRC) accurately and representatively. In this paper, the direct tensile tests (DTT) is applied, and all 5 structural specimens are extracted from a thin slab, representing UHPFRC layers covering large areas such as bridge decks and slabs or thin elements. Before processing the slab, the non-destructive test (NDT) using magnetic probe is applied to detect the local fiber content and orientation distribution of each specimen, and sequentially, predicting the tensile strength individually. For DTT, each specimen is strengthened on both ends using aluminum plates, and built-in the testing machine. By means of digital image correlation (DIC) system, the development/distribution of multiple micro-cracks and fictitious cracks of UHPFRC can be investigated visually and the propagation of each fictitious crack can be monitored from early formation until final failure.

1. INTRODUCTION

Ultra-High Performance Fiber Reinforced Cementitious Composites (UHPFRC) are composed of a highly compact cementitious matrix and a high amount of slender steel fibers, possessing extremely low permeability, high ductility and high strength. Characterized by significant strain-hardening behaviour with deformation $\varepsilon_{Utu} \geq 2‰$ and multiple fine micro-cracking (non-visible and non-detrimental) in the bulk matrix before reaching the tensile strength f_{Utu} ranging from 8 to 14MPa, the tensile behavior of good UHPFRC, in particular, is of most importance for targeted structural behavior under both serviceability and ultimate limit states. These exceptional mechanical and durability properties allows UHPFRC to be distinguished obviously from the domain of concrete, and attracts increasing interest for application of UHPFRC in the domain of built infrastructure with new design and construction concepts [1–3].

The main objective of presented study is to characterize the tensile behaviour of UHPFRC in thin slabs, representing the tensile reinforcement layer of reinforced concrete slabs or thin structural elements using UHPFRC. This is done through an extensive experimental campaign on a specific UHPFRC mix. First, an NDT method using magnetic probe, proposed by Nunes et. al [4], is applied for detecting the fiber distribution in thin slab. Second, the specimens

extracted from the slab are used for DTT. The test results are analysed regarding the fiber distribution, in particular, their influence on strain-hardening behaviour and fracture process based on visual measurement using Digital Image Correlation (DIC). Finally, the representative fiber distribution and tensile strength are proposed for a thin UHPFRC slab.

In this paper, multiple fine micro-cracking in the bulk matrix during the strain-hardening phase is defined as a "matrix discontinuity", given that this fine micro-cracking is invisible to naked eyes. The development of a discrete crack in the post-peak softening regime is called herein "fictitious crack", according to the classical definition by Hillerborg [6]. A fictitious crack shows significant stress transfer through the crack by the fibres bridging the two crack sides. An initial fictitious crack of 0.05 mm opening is visible to the naked eye. With increasing crack opening stress transfer decreases until no more stress is transferred when a crack opening of half the fiber length is reached, i.e., in present case: 6.5 mm (=*lf/2*). A crack with no more stress transfer is called herein "real crack".

2. EXPERIMENTAL CAMPAIGNS

2.1 Specimen preparation

A total of 5 structural specimens (large dumbbell specimens), extracted from a thin slab (1100mm×1100mm×50mm), were prepared for DTT, shown in Fig. 1.

The chosen UHPFRC is Holcim 707 (H707), an industrial premix containing 3.8% by volume of 13mm long straight steel fibers with diameter of 0.175mm.

The slab was cast in one step: the fresh UHPFRC mixture was placed at the center and let flow without any pulling or vibration, aimed at mimicking usual manufacturing processes for similar structural elements. Once the casting was completed, a plastic sheet was pulled over the slab to allow for auto-curing of the material. The formwork was removed 24 hours after the casting. The slab was then kept under moist curing conditions for the following seven days, and sequentially, stored inside the laboratory until testing.

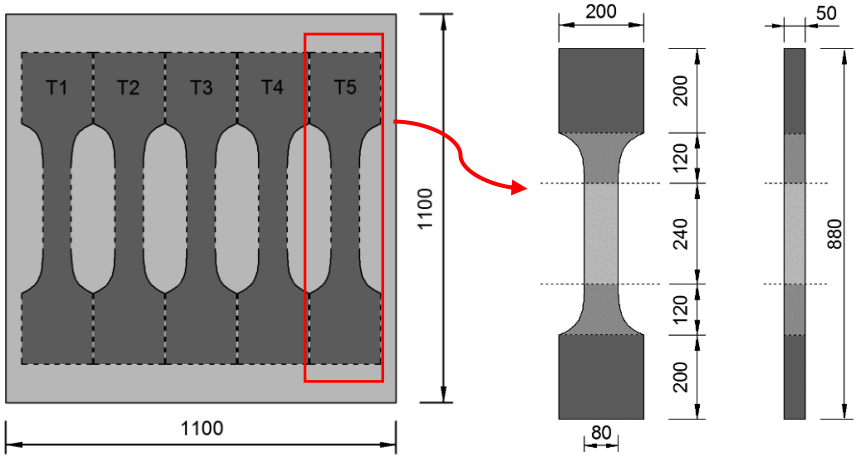

Fig.1 Extracting of dumbbell specimens & Dimension of dumbbell specimen (unit: mm)

2.2 NDT using a magnetic probe

The NDT method using magnetic probe (MP2.1), developed by FEUP (Faculdade de Engenharia Universidade do Porto) [7], is applied for inductance measurement on the whole square slab before extracting the specimens (Fig.2-a).

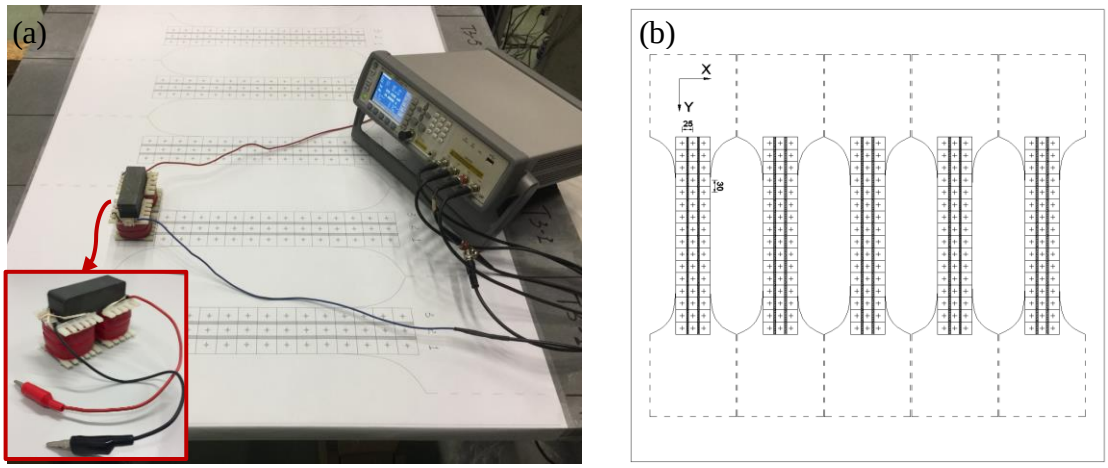

Fig.2 Inductance measurement (a) setup; (b) points location and direction

As illustrated in Fig.2-b, inductance measurement is conducted largely on the central constant area of each structural specimen on both surfaces along two orthogonal directions (X and Y). The space between each measurement point is 25mm in X direction and 30mm in Y direction (based on the size of the magnetic probe), and totally 48 pairs of measurement for each dumbbell along both orthogonal directions is carried out. The Y-direction is selected to be aligned with the tensile force direction. The inductance measurement on two directions and in the air are defined as Lx, Ly and $Lair$, respectively; and accordingly, the relative magnetic permeability in two directions is given by $\mu_{r,x} = Lx/Lair$ and $\mu_{r,y} = Ly/Lair$.

2.3 Development of DTT method

In order to largely avoid bending effect during testing, the structural specimens with head cross-section of 200mm × 50mm are built-in the testing machine by applying the principle "gluing without adherence", developed by Helbling & Brühwiler [8], as shown in Fig.3. Further details can be found in [9].

Furthermore, in order to ensure the fracture happening in the central constant part, following the idea proposed by *Graybeal et al.* [10,11], four tapered aluminum plates are affixed to two sides of both ends. Those plates have nominally thickness of 4~5mm and are tapered linearly to 1mm thickness (or as thin as possible) at tip over 50mm (Fig.4).

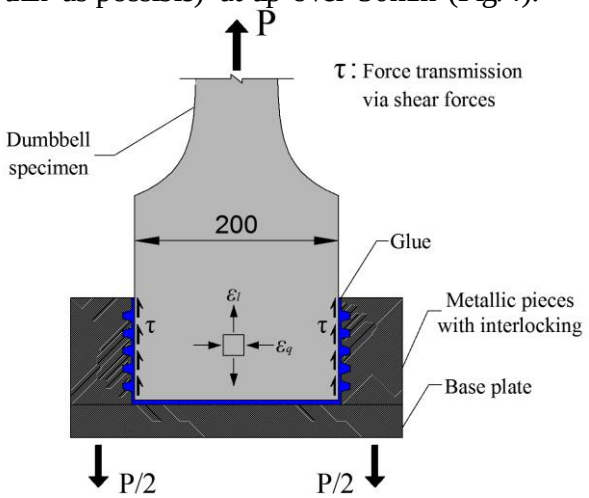

Fig.3 Built-in set-up for the tensile test at the end of specimen

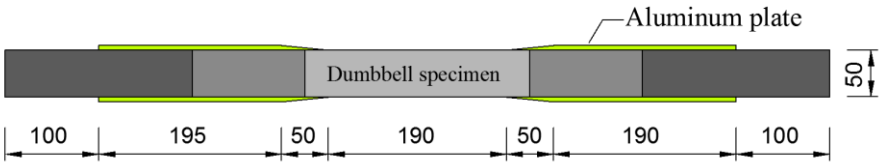

Fig.4 Dumbbell specimen affixed using 4 aluminium plates

2.4 Setup and instrumentation

The DTT is performed on a universal servo-hydraulic testing machine with a capacity of 1000kN. The DIC technique and three different series of sensors will be adopted to measure the deformation and crack opening of the UHPFRC, shown in Fig.5.

The displacement-control using the average value given by the 2 short LVDTs is applied, aiming at obtaining stable tests before and after the formation of cracks. The test speed is 0.05 mm/min in the pre-peak domain. Once the post-peak domain started, the speed will be increased to 0.1 mm/min. Regarding DIC, The shooting of the two cameras is synchronized via wired computer control with a frequency of 0.5 Hz, while 5 Hz for all the sensors

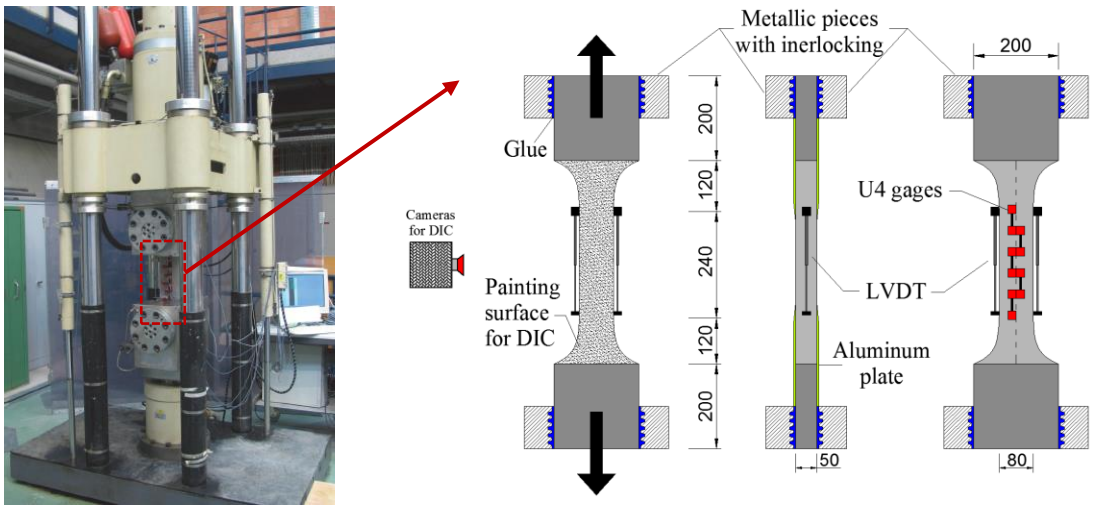

Fig.5 Tensile test setup and instrumentation for the dumbbell specimens

3. TEST RESULTS

3.1 NDT results

Based on the study from Nunes et al.[7,12], for a specific UHPFRC mix using steel fiber, the mean relative magnetic permeability ($\mu_{r,mean}$) and fiber orientation indicator ($\rho_X - \rho_Y$), both obtained from NDT measurements on two orthogonal directions, have linear relationship with fiber content (V_f) and orientation factor α_0, respectively. The corresponding definitions are given by:

$$\mu_{r,mean} = (\mu_{r,X} + \mu_{r,Y})/2 \quad (1)$$

$$(\rho_X - \rho_Y) = 0.5\frac{\mu_{r,X} - \mu_{r,Y}}{\mu_{r,mean} - 1} \quad (2)$$

Considering that the fiber content and orientation factors are both in proportion with the tensile strength of UHPFRC, as proposed by different authors [13], the contour maps with $\mu_{r,mean}(\rho_Y - \rho_X)$ are presented in Fig.6, aiming at illustrating f_{Utu} distribution qualitatively.

Obviously, randomness is observed in T2~T4, while relatively uniform and higher values are found in T1 and T5. It should be noted that a linear weak zones cross the whole section in T5, as indicated in the red circular. Thus, due to stress concentration, a lower tensile response is expected. This is also confirmed in DTT results in following section 3.2. Furthermore, the localized crack is predicted following the weak line for each specimen, as indicated by black lines in Fig.6. Those predictions are also validated in DTT results (Fig.7).

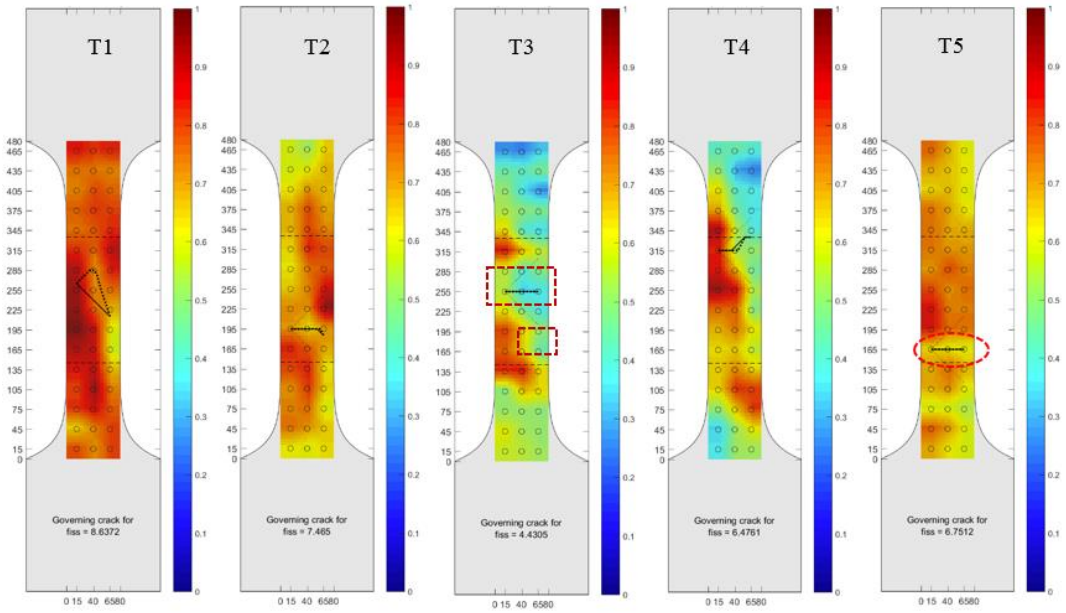

Fig.6 Contour maps with $\mu_{r,mean} \cdot (\rho_Y - \rho_X)$ (indicator of tensile strength f_{Utu}) from NDT

3.2 DTT results

3.2.1 Failure pattern

The positions of final cracks after testing for all structural specimens from DTT are presented in Fig.7, which are in good agreement with the predictions from NDT results (Fig.6). It is noted that all localized cracks occur in the central part with constant cross-section and well distribute along the flow direction of fresh UHPFRC mixture, attributed to careful design of DTT method, as described in section 2.3. Those test results, hence, can quantitatively represent the tensile peformance along the flow direction of thin slab.

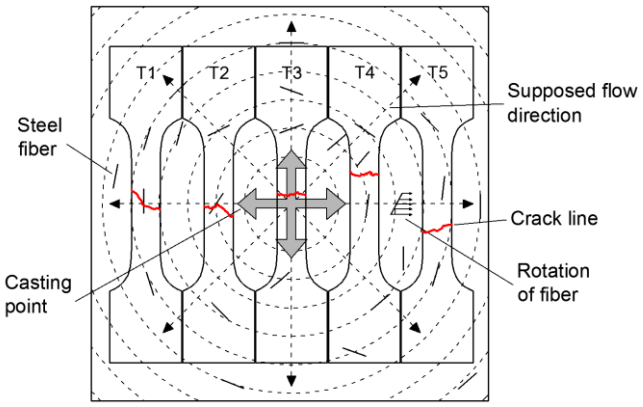

Fig.7 Schematic view of fiber orientation and crack positions of structural specimens

3.2.2 Stress-strain responses

The DTT results of five structural specimens are presented in terms of stress vs. strain (Fig. 8) curves, in which the thick black line corresponds to the average response. The stress is defined as the measured force divided by the constant cross-section area of dumbbell specimen, while the strain is based on the average value measured from two short LVDTs.

Tab.1 summarizes the main tensile parameters for each specimen, including elastic modulus E_U, elastic limit point (stress f_{Ute} and corresponding strain ε_{Ute}), and ultimate point (f_{Utu} and ε_{Utu}). Here, the end of the linear relationship in stress-strain curve is regarded as elastic limit point, and the beginning of the tensile softening response is defined as ultimate point. It is observed that all test results show similar trends: pronounced strain-hardening response with ε_{Utu} >2.0‰ (except T3-5) and f_{Utu}/f_{Ute} >1.2.

It should be noted that specimen T3-5, extracting from the similar position with T3-1, presents the lowest tensile behaviour, in particular poor strain-hardening response, compared with those results from the rests. This fact can be attributed to the locally unfavourable fiber orientation, resulting in linear weak zone through the whole cross-section, as explicated by the NDT results in section 3.2.

In general, based on the DTT results, the range of possible tensile response of UHPFRC thin slab with thickness of 50mm is presented: $9.10MPa < f_{Utu} < 12.23MPa$ and $0.68‰ < \varepsilon_{Utu} < 3.48‰$. The specimen T3-1 extracted from the edge of slab, with the longest distance from the pouring point, shows the best performance in terms of f_{Ute}, f_{Utu} and ε_{Utu}; while a strong drop (over 20%) of performance happens in specimen T3-3, extracted from the pouring point.

Tab.1 Tensile parameters from DTT

N°	E_U [GPa]	f_{Ute} [Mpa]	f_{Utu} [Mpa]	f_{Utu}/f_{Ute}	ε_{Ute} [‰]	ε_{Utu} [‰]
T3-1	45.60	9.70	12.23	1.26	0.22	3.48
T3-2	49.09	9.41	11.21	1.19	0.20	2.33
T3-3	47.39	7.74	9.62	1.24	0.17	2.68
T3-4	49.64	7.25	9.48	1.31	0.17	2.15
T3-5	48.38	7.20	9.10	1.26	0.16	0.68
Average	48.02	8.26	10.33	1.25	0.18	2.26
Std. dev.	1.59	1.21	1.33	0.04	0.03	1.02
COV	0.03	0.15	0.13	0.03	0.14	0.45

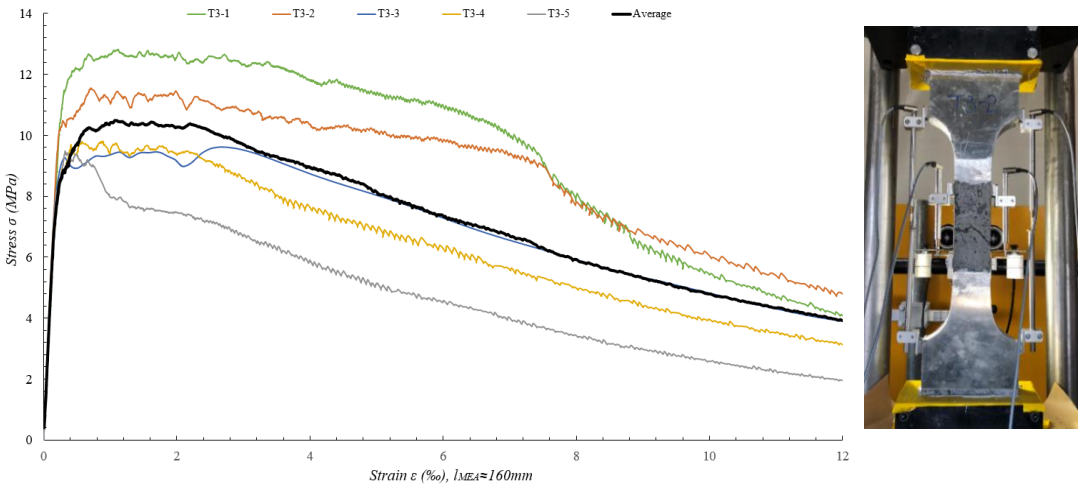

Fig.8 Tensile response of 5 structural specimens

3.2.3 Fracture process

Based on DIC analysis using VIC-3D, the whole fracture process of each specimen can be captured during loading process effectively. Particularly, the propagation of fine micro-cracks in strain-hardening domain and unloading partly in softening domain, which are invisible to naked eyes and couldn't be measured by traditional sensors, can be detected in DIC strain maps. Fig.8 shows three representative fracture processes from specimen T1, T3 and T5, respectively. In each graph, point A and B correspond to the elastic limit and ultimate limit, while point C is a random point at the end of softening branch.

In general, as illustrated in fullfiled DIC strain maps for all specimens in Fig.9-Fig.11, point A refers to the start of strain-hardening response in UHPFRC, sympolized by the activation of first fine micro-crack; while point B stands for the end of this response, characterized by the formation of single localized fictitious crack by grouping of several fine micro-cracks. After point B, the fictitious crack, where shows significant stress transfer through the fibers bridging the two crack sides, develops with increase crack opening until no more stress is transferred when a crack opening of half the fiber length is reached, i.e., in present case: 6.5 mm (=*lf/2*). And simultaneously, the rest of fine miro-cracks developing in strain-hardening domain unload partly.

However, due to the variation of fiber distribution in UHPFRC slab (as described in previous section 3.1), the strain-hardening reponse differs from different specimens. In specimen T1, with preferential alignment of fibers in loading direction, large amount of fine micro-cracks propagate in strain-hardening domain (A-B). The micro-crack pattern changes continuously as the increasing loading and has complex distribution when reaching the ultimate limit (B): many micro-cracks appear in groups, accompanied by mutiple branches; and some of them initiate seperatedly from one edge, cross each other or combine together during the propagation toward the other edge, as illustrated in Fig.9.

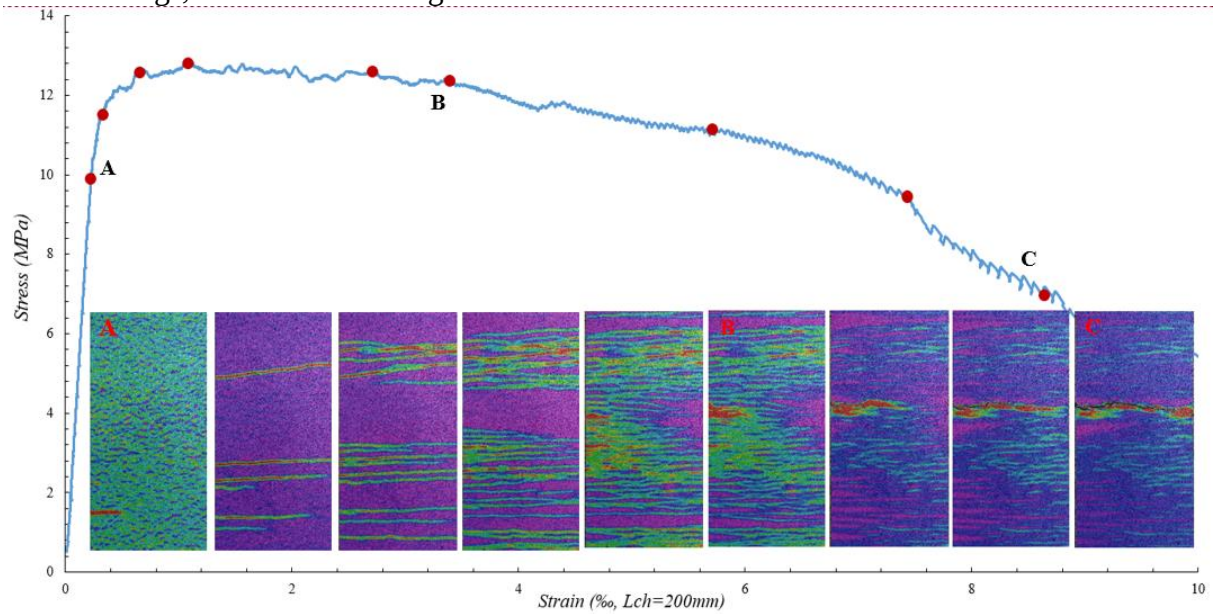

Fig.9 Fracture processes of T1

In specimen T3, where random fiber orientation distribution is assumed based on NDT analysis, less pronounced mutiple micro-cracking behavior is observed (Fig.10). Two large clusters of micro-cracks occur on the surface, and between them several micro-cracks with large

space (>*Lf*) distributed ramdonly. In this case, given that the weak areas don't pass through the whole section, the parts with prefential fiber orientation at the end of weak areas prevent the continous progation of micro-cracks initiating from those weak areas, and allow subsequent stress redistribution, characterized by appearance of new micro-cracks. However, the micro-cracks concentrated largely in the realtively weak zones, as stipulated in Fig.6-T3, resulting in lower performance compared with T1.

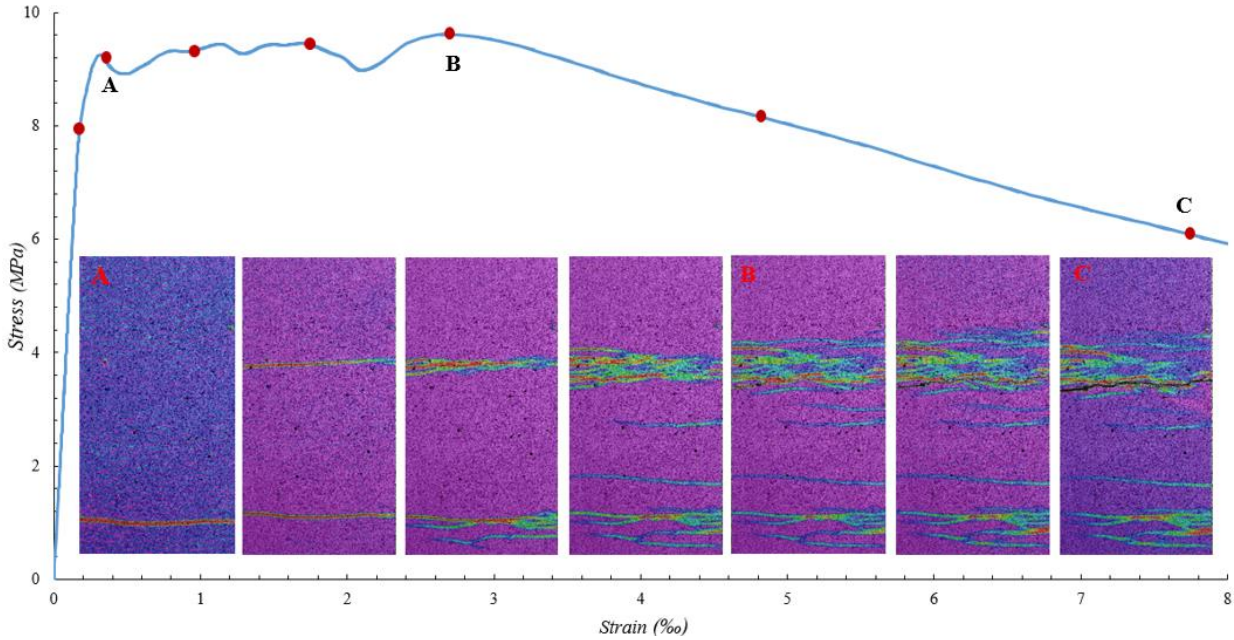

Fig.10 Fracture processes of T3

In specimen T5, the obvious weak area that crosses the section (Fig.6-T5) results in concentration of micro-cracks and subsequent fast formation of localized fictitous crack with extreme low deformation level (ε_{Utu} =*0.68‰*), see Fig.11.

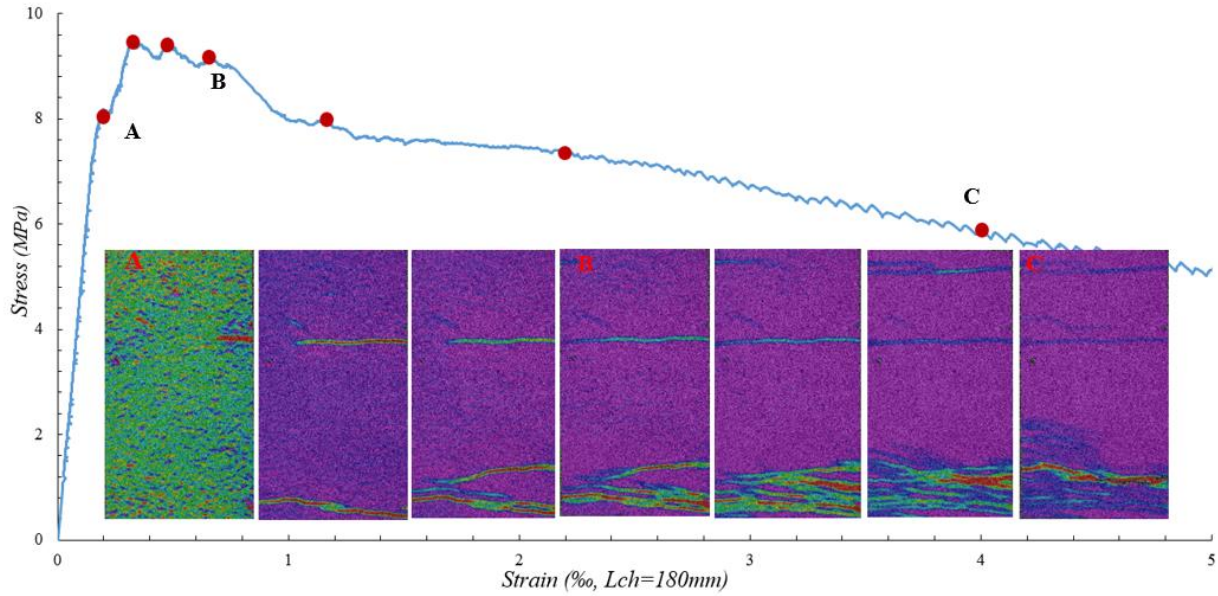

Fig.11 Fracture processes of T5

4. ANALYSIS AND DISCUSSION

4.1 Fiber distribution in thin UHPFRC slab

The considerable variation of tensile performance in the specimens extracting from different positions of the slab, suggests that the performance depends on the distance from poring point. Due to the high fluidity and workability of the UHPFRC "Holcim707©", the fresh mixture flowed freely from the center to the border in radial direction without fiber grouping or segregation, given the little difference in fiber content distribution. On the other hand, the flow exerted force on the fibers, rotating progressively the fibers perpendicular toward the flow direction, as illustrated in Fig.12. Consequentially, more fibers tend to align along the loading direction in T3-1, while 3D-uniform distribution of fibers is assumed in T3-3. This assumed radial distribution mode of fibers is consistent with previous experiment results from the author [14], and is confirmed visually by the NDT results in section 3.2, as well as the DTT results in section 3.3.

4.2 Influence of fiber distribution on tensile response of UHPFRC

Combined NDT results and DTT results, fiber distribution, especially orientation distribution, play a predominant role on mechanical behavior, in particular strain-hardening domian, of UHPFRC in tension. Tab.3 summarizes the parameters for mutiple strain-hardening behavior of each structural specimen in terms of micro-cracks number and pattern, as well as contour maps of fiber distribution from NDT for comparion. Regarding the number, the micro-cracks were counted seperately if possible, otherwise regarded as one in case they appeared in groups or very close to each other. It is obvious that more uniform fiber distribution, more micro-cracks at ultimate limit with even spacing and subsequent higher performace. As an illustrative example, specimen T1, overperformed the rests in terms of tensile response, has largest number of micro-cracks with similar small space ($\approx 4mm$, $< L_f/2$), and is closer to a homogeneous material. This can be attributed to the favourable fiber alignment in most of tested area, leading to high fiber efficiency and stress distribution in those area. With respect to random fiber distribution, like T2 and T3, some specific weak areas without passing through the whole section are found. The micro-cracks initiate from those areas, but stop continuous propagation due to the areas with preferential orientation at the end of them. This phenomena leads to certain stress distribution and initiation of micro-cracks in other weak areas. The micro-cracks, hence, concentrate largely in the realtively weak zones formed by several adjacent weak area, and consequentially, several clusters of micro-cracks in specific zones are observed. Additionally, the specimen with local weak zone (passing through the section) always results in stress concentration, accompanied by only several micro-cracks and fast formation of localized fictitious crack in this zone. Thus, very low tensile performance, deformation at f_{Utu} in particular, is reached.

Tab.2 Parameters for multiple micro-cracking behavior from NDT

N°	*Nb of micro-cracks*	*Spacing (mm)*	*Pattern*	*DIC image at f_{Utu}*	*Fiber distribution from NDT*
T1	45 ± 5	4 ± 2	Uniform	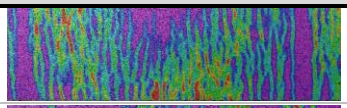	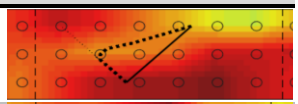
T2	20 ± 5	8 ± 2	Uniform	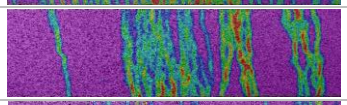	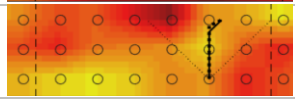
T3	12 ± 5	14 ± 2	2 Clusters	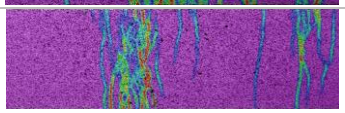	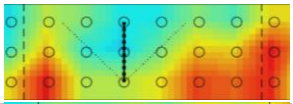
T4	10 ± 3	18 ± 4	1 Cluster	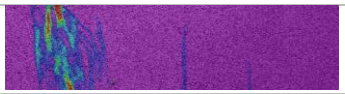	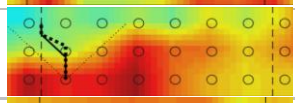
T5	6 ± 2	30 ± 5	1 Cluster	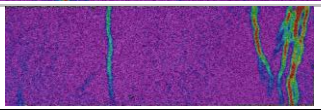	

5. CONCLUSIONS

- For a given UHPFRC mix with 3 vol.-% of fibers and good workability, the fiber distribution is uniform (showing no fiber grouping or segregation) in the thin slab. Regarding fiber orientation, the fibers have tendency to align perpendicularly toward the flow direction of fresh mixture, and a radial distribution mode of fiber orientation is rather observed in this study.
- DTT allow for characterization of the tensile response of UHPFRC. The structural specimens extracted from the slab present considerable variation in tension, suggesting significant influence of fiber orientation on tensile response, and on strain-hardening in particular. The uniform orientation distribution in UHPFRC always leads to well dispersed fine micro-cracks with similar short spacing, and subsequent high performance under tensile loading. This bestows homogeneity-like characteristics on UHPFRC material. On the contrary, the large weak zones with unfavourable fiber orientation prevent uniform stress distribution, resulting in concentration of micro-cracks in terms of clusters.
- DIC method allows identifying the fine micro-cracking development in strain-hardening domain, as well as propagation of each fictitious crack and changing crack pattern after elastic limit, thus, acting as an important basis for further study on the mechanism of damage and fracture characteristics of UHPFRC.
- NDT method using magnetic probe is promising for quick and reliable assessment of fiber content and orientation in hardened UHPFRC.

REFERENCES

[1] E. Brühwiler, Rehabilitation and strengthening of concrete structures using ultra-high performance fibre reinforced concrete, in: Concrete Repair, Rehabilitation and Retrofitting III: 3rd International Conference on Concrete Repair, Rehabilitation and Retrofitting, ICCRRR-3, 3-5 September 2012, Cape Town, South Africa, CRC Press, 2012: p. 30.
[2] E. Denarié, E. Brühwiler, Cast-on site UHPFRC for improvement of existing structures–achievements over the last 10 years in practice and research, in: 7th Workshop on High Performance Fiber Reinforced Cement Composites, 1-3, June 2015, Stuttgart, Germany, 2015.
[3] Y.L. Voo, S.J. Foster, C.C. Voo, Ultra-high performance concrete segmental bridge technology: Toward sustainable bridge construction, Journal of Bridge Engineering. 20 (2014) B5014001.
[4] S. Nunes, M. Pimentel, A. Carvalho, Non-destructive assessment of fibre content and orientation in UHPFRC layers based on a magnetic method, Cement and Concrete Composites. 72 (2016) 66–79.
[5] E. Brühwiler, "Structural UHPFRC": Welcome to the post-concrete era!, First International Interactive Symposium on UHPC - 2016. (n.d.).
[6] A. Hillerborg, Analysis of one single crack, Fracture Mechanics of Concrete (Developments in Civil Engineering). (1983) 223–249.
[7] S. Nunes, M. Pimentel, Characterization and comparison of two magnetic probes (Technical report), (2016).
[8] A. Helbling, E. Brühwiler, Eine neue Halterung für Zugversuche mit Beton-Probekörper (in German), Material Und Technik. 4 (1987) 103–107.
[9] K. Habel, Structural behaviour of elements combining ultra-high performance fibre reinforced concretes (UHPFRC) and reinforced concrete, Doctoral Thesis (EPFFL). (2004).
[10] B.A. Graybeal, F. Baby, Development of Direct Tension Test Method for Ultra-High-Performance Fiber-Reinforced Concrete., ACI Materials Journal. 110 (2013).
[11] A. Abrishambaf, M. Pimentel, S. Nunes, Influence of fibre orientation on the tensile behaviour of ultra-high performance fibre reinforced cementitious composites, Cement and Concrete Research. 97 (2017) 28–40.
[12] S. Nunes, M. Pimentel, F. Ribeiro, P. Milheiro-Oliveira, A. Carvalho, Estimation of the tensile strength of UHPFRC layers based on non-destructive assessment of the fibre content and orientation, Cement and Concrete Composites. 83 (2017) 222–238.
[13] M. Bastien-Masse, E. Denarié, E. Brühwiler, Effect of fiber orientation on the in-plane tensile response of UHPFRC reinforcement layers, Cement and Concrete Composites. 67 (2016) 111–125.
[14] X. Shen, E. Brühwiler, Tensile Behavior of UHPFRC under Uniaxial and Biaxial Stress Conditions, The 2nd ACF Symposium 2017. (2017).